Korean J. Chem. Eng., 34(4), 1222-1228 (2017)
DOI: 10.1007/s11814-016-0361-6

pISSN: 0256-1115
eISSN: 1975-7220

Effect of high molecular weight isocyanate contents on manufacturing polyurethane foams for improved sound absorption coefficient

Giwook Sung and Jung Hyeun Kim†

Department of Chemical Engineering, University of Seoul, 163 Siripdaero, Dongdaemun-gu, Seoul 02504, Korea
(*Received 14 October 2016 • accepted 23 December 2016*)

Abstract−Noises generated in automobile compartments can be controlled by utilizing sound absorption and insulation materials such as polyurethane foams. Polyurethane foams are synthesized by varying polymeric methylene diphenyl diisocyanate (MDI) content for exploring the effect of high functional isocyanate on cellular and acoustic properties. The use of polymeric MDI affects polyurethane matrix modulus and drainage flow rate of the foams, and it also has strong effects on cell structure and air flow resistance (AFR). The highest sound absorption coefficient is achieved at the optimum amount of the polymeric MDI. Therefore, the optimum amount of polymeric MDI content is recommended to achieve not only high sound absorption coefficient but also high transmission loss from the polyurethane foams.

Keywords: Polyurethane Foam, Multifunctional Isocyanate, Cell Morphology, Sound Absorption

INTRODUCTION

Noise pollution has been a serious problem with growing numbers of automobiles, and it is becoming a major concern in purchasing automobile products for comfortable driving environments. Automotive noise pollution generally consists of the structure-borne and airborne noises from driving conditions. For this reason, the sound absorption efficiency is crucial in designing automotive interior materials [1,2]. A notable portion of the structure-borne noise occurs in the low frequency regime (30 to 500 Hz), and airborne noise occurs in medium and high frequency regimes (500 to 8,000 Hz) [3]. These noises can be prevented from driving systems by using sound absorption materials. Generally, stacked piles of sound absorption and insulation materials are used to control noises from leaked and reflected sounds. Among various noise controlling materials, polyurethane foams have a wide range of applications because of high sound absorption efficiency and easy production. Various studies have been reported utilizing various fillers for polyurethane composite foams as a sound absorption material [4-7]. Sung et al. [4] proposed improved sound absorption efficiency of polyurethane composite foams including plate-like fillers, and Verdejo et al. [5] also reported the effect of carbon nanotube on sound absorption efficiency of polyurethane foams. In addition, micron-size [6] and nano-size fillers (silica and clay) [7] were also used for obtaining higher sound absorption efficiency of polyurethane foams. Besides sound absorption applications, a few results as an insulation material were reported utilizing rice-hull fillers for polyurethane composite foams [8].

In addition to the usage of fillers to improve acoustic properties of polyurethane foams, various ingredients in fabricating polyurethane foams are crucial for modulating cell morphology on enhancements of sound absorption efficiency [9]. Isocyanate is an especially key component in polyurethane polymerization, and thus the type of isocyanate molecular structure is crucial to obtain desired cavity and pore sizes. The isocyanate structure affects the reaction rate and drainage flow rates during cell formation to form polyurethane struts and walls. Physical properties of the polyurethane foams can also be influenced by experimental foaming processes, such as one-step and pre-polymer methods.

In this study, we fabricated polyurethane foams with various amounts of polymeric MDI which contains multiple NCO functional groups. Multiple NCO functionalities of polymeric MDI help to form networks in polyurethane foam matrix, and so it leads to the decrease of drainage flow rate at high content of polymeric MDI. Morphological properties such as cavity and pore sizes and open porosity are strongly dependent on the ratio of polymeric MDI to the isocyanate mixture. Therefore, the effect of polymeric MDI content on the acoustic behaviors was investigated by analyzing morphology and air flow resistance of the polyurethane foams. For morphological analysis, the image pro-plus software was utilized for scanning electron microscopy images to obtain average results of the cavity and pore sizes as well as open porosity.

EXPERIMENTAL

1. Materials

Polyurethane foams were manufactured using a polyether based polyol (KE-810, KPX Chemical, OH value 28±2, $M_W \fallingdotseq 6{,}000$ g/mol, average functionality (f_{av})=3) and two types of isocyanate. The isocyanates are KW 5029/1C-B (%NCO 35±0.5, BASF) and COSMONATE SR500 (%NCO 31±0.5, Kumho Mitsui Chemicals). KW 5029/1C-B consists of 70% monomeric MDI, 12.5% polymeric MDI, and 17.5% toluene diisocyanate in mole per grams. The average numbers of NCO groups per molecule are close to 2.0 for KW

†To whom correspondence should be addressed.
E-mail: jhkimad@uos.ac.kr

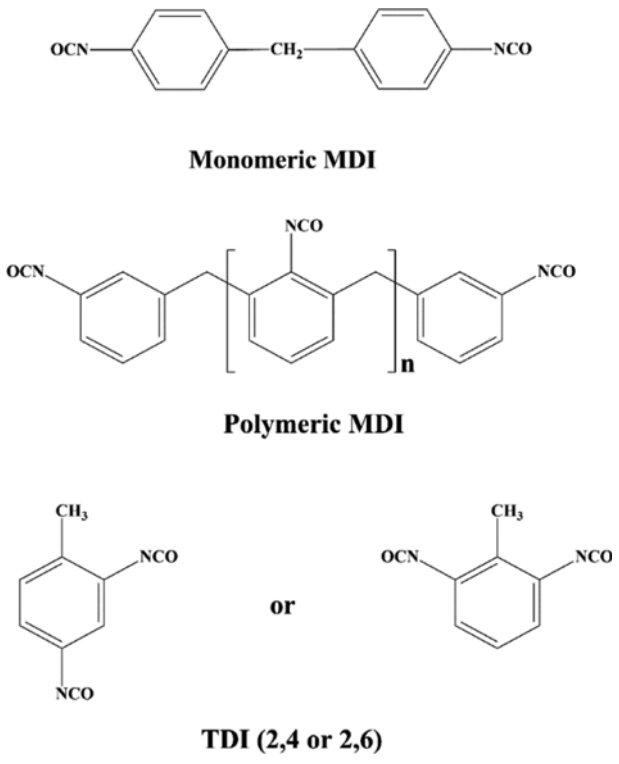

Fig. 1. Chemical structure of various isocyanates.

5029/1C-B and 2.85 for COSMONATE SR500 (polymeric MDI mixture), respectively. Therefore, the number of NCO groups per molecule in the isocyanate mixture can be controlled by varying the mixing ratio of both isocyanate components. Viscosities of KW 5029/1C-B and COSMONATE SR500 are 0.2 and 5.0 g cm^{-1} s^{-1} at 25 °C.

Fig. 1 shows the individual molecular structures of the three types of isocyanates used in this study. BL11 (70% bis(2-dimethylaminoethyl) ether (BDMAEE) diluted with 30% dipropylene glycol) and Dabco 33LV (33% triethylenediamine (TEDA) and 67% dipropylene glycol) were used as blowing and gelling catalysts from Air products and Chemicals. Diethanolamine (DEA) was used as a cross-linking agent, and de-ionized water (H_2O) was used as a blowing agent. Silicon surfactant L-3002 (Momentive Corp) was used for stabilizing cavities and interconnecting pores in the foams.

2. Synthesis

Bulk polymerization without a pre-polymer synthesis step was performed in an aluminum mold (400×400×30 mm^3). First, the pre-mixture systems (containing polyol, chain extender, gelling and blowing catalyst, H_2O, and silicon surfactant) were weighed in a 400 mL paper cup and mixed with a mechanical stirrer (EURO STAR 20, IKA) for 20 min at 1,700 rpm. Second, the weighed isocyanate mixtures were added to the pre-mixture systems and mixed further for 10 s at 6,000 rpm. After the mixing process, the final mixtures were poured into the mold, and the mold was tightly clamped with the mold cover and kept at 60 °C for 10 min. Detailed formulations are shown in Table 1 by considering the mold volume. For example, 42 g of polymeric MDI in the first formulation can be obtained from 21 g of SR-500 (100 wt% polymeric MDI) and 166 g of KW5029/1C-B (12.5 wt% polymeric MDI).

Table 1. The formulations of various polyurethane foams

Ingredient	Formulation (g)*				
Polyol (KE-810)	300				
Isocyanate A (SR-500)	21	42	62	83	104
Isocyanate B (KW5029/1C-B)	166	147	129	110	92
Polymeric MDI contents	42	60	78	97	115
L-3002			3.96		
BL-11			0.24		
Dabco 33LV			2.16		
DEOA			1.8		
Water			12		

*NCO Index: 1.0

The isocyanate content was calculated by keeping the NCO index as 1.0, as reported elsewhere [10]. All polyurethane foams were fabricated at room temperature and 50±10% relative humidity, and they have average density about 60±10 kg/m^3.

3. Morphology

Cellular structures of cavities and interconnecting pores were examined with scanning electron microscopy (SEM, SNE-3000M, SEC Co. Ltd., at 30 kV). The samples for SEM measurements were treated with a gold film sputter (MCM 100, SEC Co. Ltd.), and the operational power was 30 kV. SEM samples were prepared from the mold foams in several different locations. Approximately 10 SEM images and Image Pro Plus software were used in analyzing sizes of the cavities and pores and types of pores (open, partial-open, close). A typical image including open, partially open, and close pores is shown in Fig. 2, and the cavity structure in the polyurethane foam is also noted in the image.

4. Air Flow Resistance

Air flow resistance (R_S, AFR) is a physical property showing pressure drop related to the amount of material porosity. AFR was measured to understand the propagation of sound waves through polyurethane foams with the air flow resistance system device (Autoneum Holding Ltd., Switzerland). AFR measurements were per-

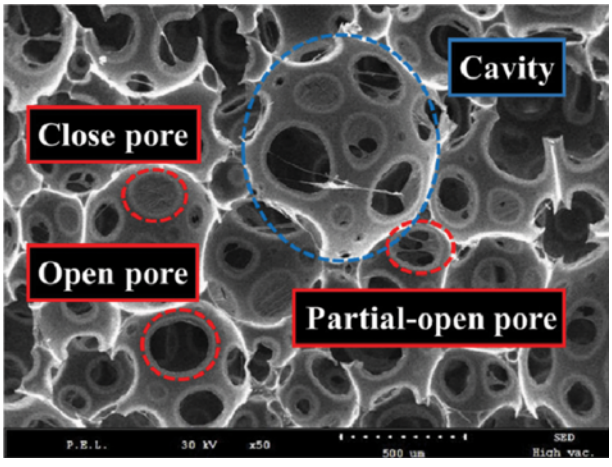

Fig. 2. SEM image defining areas for cavity and three types of pores (open, partial-open and close).

formed following ASTM C522-03 at 0.042 m/s air flow rate and room temperature. The results were analyzed using the VECTOR software following the equation:

$$R_s = [kg/s \cdot m^2] = \frac{\Delta P}{q_v} \times A, \quad (1)$$

where ΔP [kg/s^2·m], q_v [m^3/s] and A denote pressure difference, volumetric airflow rate, and cross sectional area.

5. Thermo-mechanical Properties

Dynamic mechanical analyzer (DMA, Q800, TA instruments, USA) was used in a compression mode to measure glass transition temperature of polyurethane foams. Cylindrical samples were manufactured as 0.8 cm thickness and 4 cm diameter. Operating frequency and amplitude were maintained within 1 Hz and 40 μm, respectively. Scanning temperature ranged from −70 °C to 20 °C with a heating rate of 5 °C per min. Tan δ representing the glass transition temperature of samples was calculated by measuring response energies from applied oscillating stress of the samples.

6. Acoustic Properties

Sound absorption property of polyurethane foams was measured by the impedance tube method (Type 7758, B&K Korea) at room temperature. The sound absorption analysis was performed following the ASTM E1050-12 based on the transfer function method. The measurements were done for each sample in the frequency range from 160 Hz to 6,300 Hz with two 1/4 inch microphones. The sample thickness was 20 mm, and the sample diameters for high (500-6,300 Hz) and low frequency (160-800 Hz) measurements were 30 and 100 mm, respectively. The sound absorption was obtained by combining low and high frequency results using the Pulse and VA-LAB4 software for single range plots.

7. Compression Strength

The compression strength was measured at room temperature using a universal test machine (UTM, LS1, Lloyd Instruments Ltd.) according to ASTM D395-16 at a crosshead speed of 100 mm min^{-1}. The cylindrical sample dimension for the compression test was 60 mm in diameter with 20 mm thickness. The compression tests were performed for 70% strain condition.

RESULTS AND DISCUSSION

1. Morphology

Cellular morphology is closely related to the physical and acous-

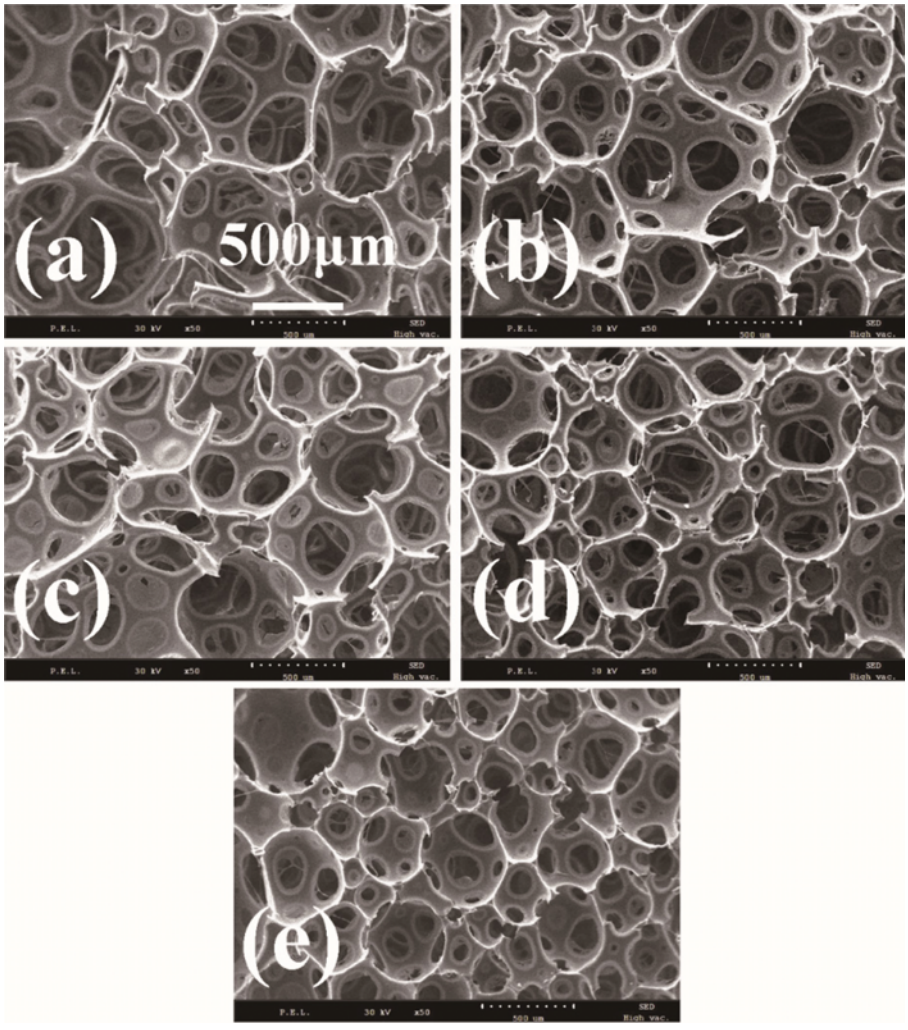

Fig. 3. SEM images of polyurethane foams with various polymeric MDI content (g): 42 (a), 60 (b), 78 (c), 97 (d), 115 (e).

tic properties because porosity and cavity sizes significantly affect the material density and air propagation through materials [11]. Fig. 3 shows SEM images for the variation of cavity and pore sizes with increasing polymeric MDI mole per grams in polyurethane systems, and cavity and pore sizes are decreasing with increasing the polymeric MDI contents. It could be attributed to the increased matrix viscosity and modulus resulting from high crosslinking reaction with the increased polymeric MDI content.

For example, increased matrix viscosity with polymeric MDI induces decreased drainage flow rate during polymerization, and it thus gives unfavorable condition for cavities and pore formation [9,12]. In addition, high crosslinking density of polyurethane matrix produced from high functional polymeric MDI further improves the modulus of polyurethane matrix during blowing reaction. Therefore, use of multifunctional polymeric MDI in fabrication of polyurethane foams affects significantly the formation of the cellular morphology.

In more details, Fig. 4 shows the cavity and pore diameters, open porosity, and relative ratio of the pore types. As the similar demonstration above in Fig. 3, the average diameters of cavity and pore are decreasing about 28% and 44%, respectively, as shown in Fig. 4(a) and 4(b). Higher decrement of pore sizes is possibly due to the sequential formation mechanisms of cavity and pores, and the change of pore sizes also influences on air flow resistance, which is closely associated with collisions of sound waves with the cell walls and struts.

Typically, the interconnecting pores are formed simultaneously or after the cavity formation [13], and so pore interconnection is significantly affected by the viscosity and modulus of matrix material. In addition, the relative number of pore types is strongly related to the airflow resistance and open porosity. The open porosity was also analyzed following Eq. (2) [14]:

$$\text{Open porosity}=(N_o+N_p\times 0.5)/(N_o+N_p+N_c), \quad (2)$$

where N_o, N_p, N_c are the number of open, partial-open, and close pores. Fig. 4(c) also shows the decreasing tendency of porosity with increasing polymeric MDI content, and it is again possibly due to the high possibility of presence of closed pores at high viscosity and modulus of matrix. Fig. 4(d) presents the relative ratios of open, partial-open, and close pores as a function of polymeric MDI content. Contrary to decreasing tendency of the open pores, the relative ratios of partial-open and close pores are increasing with polymeric MDI content. In addition, at the highest polymeric MDI content, porosity (Fig. 4(c)) and relative pore ratio (Fig. 4(d)) showed large uncertainties due to the high viscosity delocalization in isocyanate mixtures. This morphological result is intrinsically related to the following sound absorption property.

Considering the morphological images and results of cavity and pore analysis shown in Figs. 3 and 4, schematic illustrations of cavity and pore formation mechanisms are shown in Fig. 5. In cavity formation, relative intensity between matrix modulus and CO_2 gas pressure can determine the final cavity sizes. With increasing polymeric MDI content, cavity growth can be limited due to the high resistance by the increased matrix modulus. Gaefke et al. [15] also reported the effect of increased viscosity of polyurethane polymer by high crosslinking density of polyurethane foams on the matrix modulus. In pore formation, drainage flow can be a dominating factor in competing with the CO_2 gas pressure generated inside the cavities, and thus low drainage flow can result into the high number of closed pores at high polymeric MDI content. Therefore, inclusions of high molecular weight isocyanate with high functionalities have a significant effect on formation of cavity and interconnect-

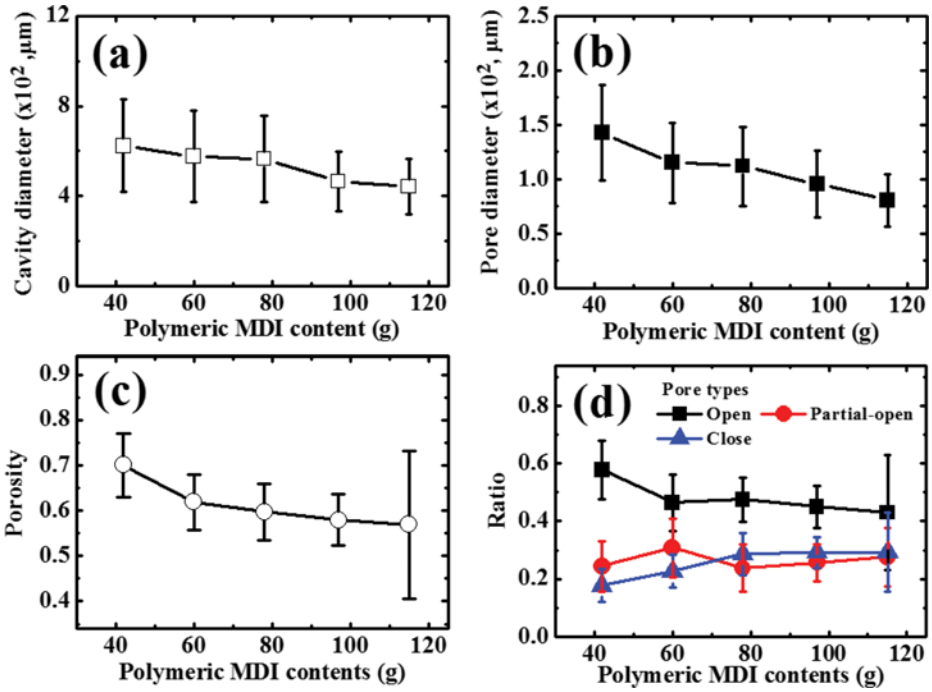

Fig. 4. Cavity diameter (a), pore diameter (b), porosity (c), relative ratio of various pore types (d) with increasing polymeric MDI content (g).

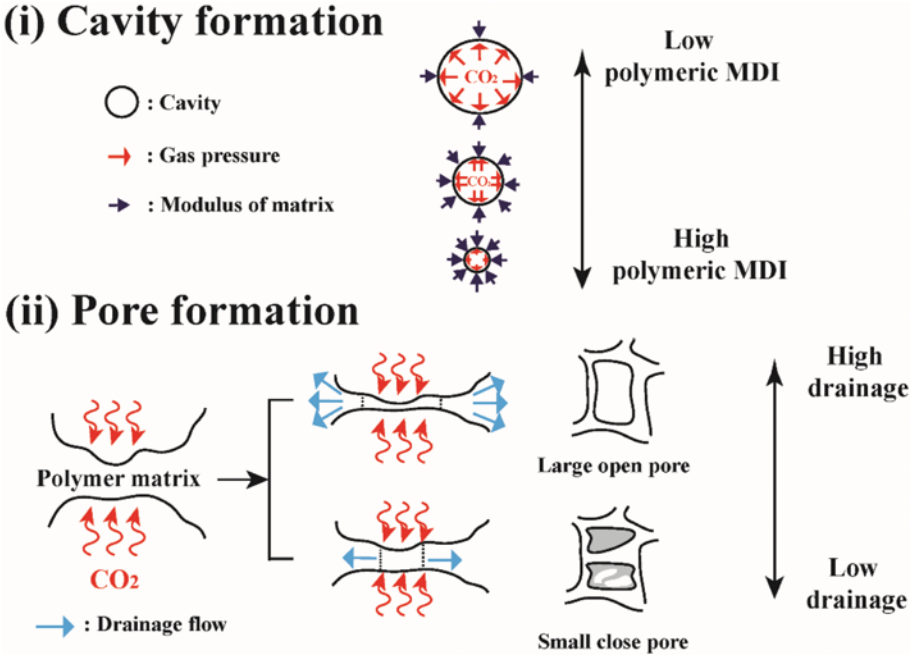

Fig. 5. Scheme of viscosity effects on cavity and porosity.

ing pores in polyurethane foams.

2. Air Flow Resistance

Air permeation through pores and friction between sound wave and cell wall are strongly related to morphological properties of porous materials, and they can be predicted with AFR measurements. The higher the AFR value is, the more collisions between sound energy and polyurethane matrix occur. In general, AFR increases with decreasing the porosity of porous materials [16]. Fig. 6 shows AFR results as a function of polymeric MDI content, and it increases with increasing the polymeric MDI content. The AFR was about 300 kg s^{-1} m^{-2} at 42 g of polymeric MDI content, and it increased drastically to 5×10^4 kg s^{-1} m^{-2} at 115 g of polymeric MDI content. It is about 160 times higher than 42 g case, and it is surely due to the decreased porosity and cell size, as shown in Fig. 4. This increased AFR also represents the difficulty in air and wave propagation through the pores, and thus it can be used to translate the increment in sound absorption coefficient.

3. Dynamic Mechanical Analysis

Varying the content of high functional isocyanate in the isocyanate mixture, final polyurethane foams are subjected to different viscoelastic response under applied stress condition. The nature of this response can be used to determine the storage and loss moduli of material, and it can also be closely related to the glass transition temperature (T_g) of the material. In DMA, tan δ is defined as the ratio between the loss modulus and the storage modulus, and it represents T_g counting the relative contribution of the viscous and elastic properties. In addition, the area under the tan δ curve is strongly associated with damping property of materials. As reported in several studies, the improved damping property with large area under the tan δ curve showed increased sound absorption effi-

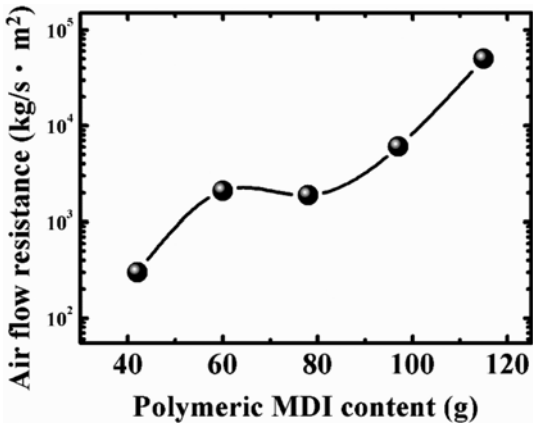

Fig. 6. Air flow resistance with polymeric MDI content (g).

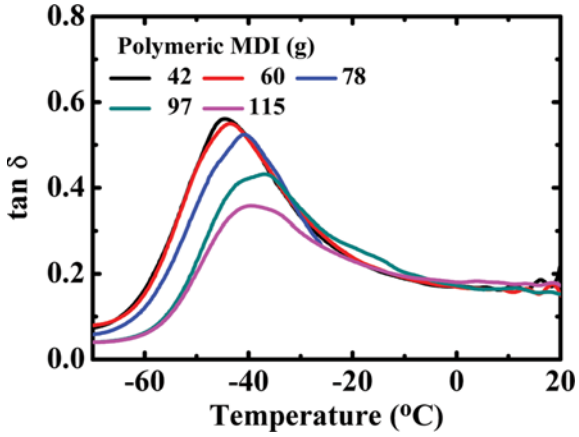

Fig. 7. Tan δ of polyurethane foam with various polymeric MDI content (g).

ciency [17-19].

Fig. 7 shows the results of tan δ measurements for various polymeric MDI content as a function of temperature. As the polymeric MDI content was increased, the tan δ peak moved to higher temperature, while the area under the curve decreased. It could be due to the decreased mobility of polyurethane chains by high cross-linking possibility from multifunctional isocyanate groups. This decreasing area under the tan δ curve with increasing the polymeric MDI content possibly indicates the difficulty of losing energy by molecular rearrangements and internal frictions, and thus it can further influence the reduction of sound absorption coefficients.

4. Sound Absorption Efficiency

Non-acoustic parameters such as cell morphology, stiffness of cell walls, and environmental conditions determine the resulting efficiencies of sound absorption through polyurethane foams [7, 17,20-23]. The sound absorption property results from two major sound absorption mechanisms: friction of air molecules with sound energy, collision of sound waves with polyurethane matrix. For this reason, the sound absorption coefficient could be efficiently analyzed by using AFR measurements [8]. In automotive applications, the sound absorption materials are crucial in reducing reflected sound energy from secondary noises.

Fig. 8(a) shows the sound absorption coefficient, and Fig. 8(b) represents the noise reduction coefficient (NRC, arithmetic mean of absorption coefficients at 250, 500, 1000, and 2,000 Hz), which is generally used for interpretation of the sound absorption [24-26].

Considering the AFR results in Fig. 6, the sound absorption of the foams is low at low AFR values, but it reaches a maximum value at 60 g of polymeric MDI content as increasing the AFR. After the maximum point, it starts to decrease with further increasing AFR because little sound energy can be absorbed through interior cells with increased difficulty of wave penetration at high AFR with low open porosity. In addition, the AFR effect on sound absorption coefficient, decreased damping property at high polymeric MDI content can cause reduction of sound absorption, as revealed in tan δ curves in Fig. 7. This reduced damping phenomenon showed a negative effect on the sound absorption by decreased collision possibility of sound waves with polyurethane matrix. In addition, the sound absorption coefficient results showed two distinct regimes: low (160-1,500 Hz) and high (1,500-6,300 Hz) frequency ranges. In low frequency region, the sound absorption coefficient increased with increasing the polymeric MDI content, and it is possibly due to the resonance effects of polyurethane foams with reduced vacant volume, including small cavity sizes, as mentioned in several studies [27,28]. On the contrary, in high frequency region, the sound absorption coefficient generally decreased with increasing the polymeric MDI content due to the decreased damping effect. From these results, optimum amount of polymeric MDI content (60 g) is recommended to achieve high sound absorption coefficient.

5. Compression Strength

For applications of polyurethane foams in sound absorption materials, it is important to maintain their physical strength for long-term usages [10,29]. The compression strength as a function of polymeric MDI in the isocyanate is shown in Fig. 9. The physical strength of foams is strongly related to the foam morphology. The compression strength increases with increasing the polymeric MDI contents and it could be due to the reduced cavity and pore sizes and due to the decreased porosity, as mentioned in the morphological analysis section (Fig. 4). The decrease of cavity and pore sizes can lead to the increase of strut size, which can act as a robust supporting wall, and decreased porosity can also generate a high number of partially open and closed pores for increased foam strength. In addition, increased T_g from tan δ curves (Fig. 7) at high polymeric MDI content also improves the compression strength and possibility of long term usages of the polyurethane foam products. Therefore, improved compression strength with high content

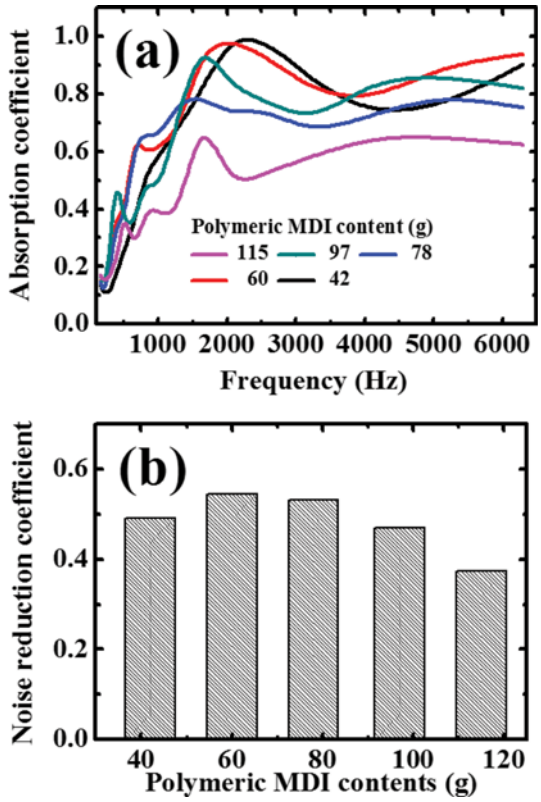

Fig. 8. Sound absorption coefficient (a) and noise reduction coefficient (b) with various polymeric MDI content (g).

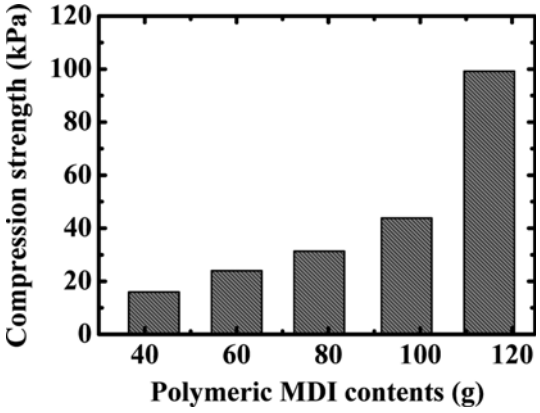

Fig. 9. Compression strength as a function of polymeric MDI content (g).

of the polymeric MDI is promising in applications of polyurethane foams for automotive sound absorption materials.

CONCLUSIONS

Polyurethane foams were fabricated with various polymeric MDI content for exploring the effect of isocyanate functionality on the cell morphology and acoustic property. As increasing the polymeric MDI contents, cavity and pore sizes of the foams were decreased not only by the increased polyurethane matrix modulus but also by the low drainage flow rate. The reduced flow also decreased the open porosity of the foams. These morphological changes from the increased polymeric MDI content increased the air flow resistivity drastically about 160 times. This high AFR directly improved the sound absorption coefficient because of the difficulty in wave penetration. The sound absorption coefficient was low at low AFR values, but it reached a maximum value as the AFR further increased. After the maximum point, sound absorption decreased with increasing AFR because little sound energy could be absorbed through interior cells at too high AFR. Therefore, the optimum amount of polymeric MDI content is recommended to achieve a high sound absorption coefficient from the polyurethane foams.

ACKNOWLEDGEMENT

This research was supported by a grant (No. 201506112002) from Hyundai-NGV.

REFERENCES

1. J.-W. Lee, J.-C. Lee, J. Pandey, S.-H. Ahn and Y. J. Kang, *J. Compos. Mater.*, **44**, 1701 (2010).
2. M. Saha, M. E. Kabir and S. Jeelani, *Mater. Sci. Eng., A*, **479**, 213 (2008).
3. N. Park, Y. Kim and C. Park, *Chemistry*, **8**, 197 (1997).
4. C. H. Sung, K. S. Lee, K. S. Lee, S. M. Oh, J. H. Kim, M. S. Kim and H. M. Jeong, *Macromol. Res.*, **15**, 443 (2007).
5. R. Verdejo, R. Stämpfli, M. Alvarez-Lainez, S. Mourad, M. Rodriguez-Perez, P. Brühwiler and M. Shaffer, *Compos. Sci. Technol.*, **69**, 1564 (2009).
6. H. Zhou, B. Li and G. Huang, *J. Appl. Polym. Sci.*, **101**, 2675 (2006).
7. R. Gayathri, R. Vasanthakumari and C. Padmanabhan, *Int. J. Sci. Eng. Res.*, **4**, 301 (2013).
8. Y. Wang, C. Zhang, L. Ren, M. Ichchou, M. A. Galland and O. Bareille, *Polym. Compos.*, **34**, 1847 (2013).
9. J. G. Gwon, G. Sung and J. H. Kim, *Int. J. Precis. Eng. Manuf.*, **16**, 2299 (2015).
10. G. Sung, S. K. Kim, J. W. Kim and J. H. Kim, *Polym. Test.*, **53**, 156 (2016).
11. J. G. Gwon, S. K. Kim and J. H. Kim, *J. Porous Mater.*, **23**, 1 (2015).
12. Z. Lan, R. Daga, R. Whitehouse, S. McCarthy and D. Schmidt, *Polymer*, **55**, 2635 (2014).
13. S.-T. Lee and N. S. Ramesh, *Polymeric foams: mechanisms and materials*, CRC Press, New York (2004).
14. C. Zhang, J. Li, Z. Hu, F. Zhu and Y. Huang, *Mater. Des.*, **41**, 319 (2012).
15. C. Gaefke, E. Botelho, N. Ferreira and M. Rezende, *J. Appl. Polym. Sci.*, **106**, 2274 (2007).
16. R. del Rey, J. Alba, J. P. Arenas and V. J. Sanchis, *Appl. Acoust.*, **73**, 604 (2012).
17. J. Lee, G. H. Kim and C. S. Ha, *J. Appl. Polym. Sci.*, **123**, 2384 (2012).
18. N. Najib, Z. M. Ariff, A. Bakar and C. S. Sipaut, *Mater. Des.*, **32**, 505 (2011).
19. K. P. Menard, *Dynamic mechanical analysis: a practical introduction*, CRC Press, New York (2008).
20. J. G. Gwon, S. K. Kim and J. H. Kim, *Mater. Des.*, **89**, 448 (2016).
21. C. Zhang, Z. Hu, G. Gao, S. Zhao and Y. Huang, *Mater. Des.*, **46**, 503 (2013).
22. O. Doutres, N. Atalla and K. Dong, *J. Appl. Phys.*, **110**, 064901 (2011).
23. M. Álvarez-Láinez, M. A. Rodríguez-Pérez and J. A. de Saja, *Mater. Lett.*, **121**, 26 (2014).
24. G. C. Gardner, M. E. O'Leary, S. Hansen and J. Sun, *Appl. Acoust.*, **64**, 229 (2003).
25. S. Fatima and A. Mohanty, *Appl. Acoust.*, **72**, 108 (2011).
26. S. Huda, N. Reddy and Y. Yang, *Composites Part B.*, **43**, 1658 (2012).
27. X. Zhang, Z. Lu, D. Tian, H. Li and C. Lu, *J. Appl. Polym. Sci.*, **127**, 4006 (2013).
28. Z. Hong, L. Bo, H. Guangsu and H. Jia, *J. Sound Vib.*, **304**, 400 (2007).
29. H. Lim, S. Kim and B. Kim, *Express Polym. Lett.*, **2**, 194 (2008).